Research Square

Preprints are preliminary reports that have not undergone peer review.
They should not be considered conclusive, used to inform clinical practice,
or referenced by the media as validated information.

Digital Enrichment of Hyperthermophilic Archaeal Viruses from a Natural Hot Spring Reveals Local Diversification in Response to Host CRISPR-immunity

Rachel Whitaker

rwhitakr@illinois.edu

University of Illinois at Urbana Champaign https://orcid.org/0000-0003-2263-5798

Thomas Cowell

University of Illinois Urbana-Champaign

Changyi Zhang

University of Illinois at Urbana-Champaign

Jiayue Yang

University of Illinois Urbana-Champaign

Chih-Lin Chen

University of Illinois Urbana-Champaign

Mark Young

Montana State University

Hee-Sun Han

University of Illinois Urbana-Champaign

Article

Keywords:

Posted Date: April 6th, 2026

DOI: https://doi.org/10.21203/rs.3.rs-9151609/v1

License: This work is licensed under a Creative Commons Attribution 4.0 International License.
Read Full License

Additional Declarations: There is **NO** Competing Interest.

Digital Enrichment of Hyperthermophilic Archaeal Viruses from a Natural Hot Spring Reveals Local Diversification in Response to Host CRISPR-immunity

Thomas W. Cowell[1,2,3†], Changyi Zhang[1,2†], Jiayue Yang[1,2], Chih-Lin Chen[3], Mark Young[4], Hee-Sun Han[1,3*], Rachel J. Whitaker[1,2*]

[1] Carl R. Woese Institute for Genomic Biology, University of Illinois Urbana-Champaign, Urbana, Illinois 61801, USA

[2] Department of Microbiology, University of Illinois Urbana-Champaign, Urbana, Illinois 61801, USA

[3] Department of Chemistry, University of Illinois Urbana-Champaign, Urbana, Illinois 61801, USA

[4] Department of Microbiology and Immunology, Montana State University, Bozeman, Montana 59717, USA

[†]These authors contributed equally.

*****Correspondence should be addressed to: Rachel J. Whitaker (rwhitakr@illinois.edu) or Hee-Sun Han (hshan@illinois.edu)

Abstract:

Despite recent advances in metagenomics, recovering the strain-level diversity of viral communities remains a challenging and laborious process. Metagenomic sequencing approaches are limited by incomplete genome assembly and low coverage for all but the most abundant viral species in a sample. Here, we extend droplet microfluidic cultivation techniques facilitate targeted enrichment of the archaeon *Sulfolobus* (now *Saccharolobus*) *islandicus* and its associated lytic virus *S. islandicus* rod-shaped virus (SIRV) to enhance viral metagenomics. By compartmentalizing the natural diversity of a Yellowstone hot spring sample into single virus droplets, we eliminate inter-strain competition and preserve population-level diversity during enrichment of the focal viral species. Sequence analysis of enriched metagenomes confirmed that selective enrichment recovered mostly SIRVs, while drop-compartmentalization outperformed a traditional liquid culture to recover the deep local diversity of a lytic viral population from a

natural hot spring. Analysis of SIRV variants revealed selective forces shaping the viral population, including local adaptation in response to host CRISPR-immune selection for viral escape mutations.

Introduction:

Given their abundance and ubiquity, microbial viruses shape ecological and environmental processes across terrestrial, aquatic, and host-associated microbiome environments.[1–4] Viruses structure microbial communities through lysis and participate in horizontal gene transfer and symbioses, extending phenotypes of microbial cells to be toxic, resistant, or fast or slow growing.[5–7] Despite rapid advances in sequencing length and depth, there are limited tools to study relevant strain-level diversity needed to capture virus-host dynamics in microbial populations. Therefore, given the vast diversity and invisible complexity of microbial scales, multiscale eco-evolutionary dynamics of microbial viruses and how they feed back on ecosystem stability, diversity, and change over time and space remain obscure.[8,9]

To sample the natural strain-level viral diversity, we developed a single virus enrichment platform where each drop in an emulsion containing growing bait host acts as an individual isolated environment for each viral strain. Unlike in a typical bulk enrichment culture, this approach prevents competition among viral strains and removes the enrichment bias towards those viruses that happen to infect and replicate fastest on the chosen bait host. We demonstrate the value of this approach using droplet-enriched metagenomes to explore patterns of viral diversity associated with selection by CRISPR-Cas immunity in a model hot spring population.

We focus on extreme aquatic environments as a well-defined population where changes in allelic diversity can be linked to changes in local viral populations. Unlike many microbial systems, hot springs have clear boundaries, defined geochemical composition, and constrained species and viral diversity.[10–12] The culturable and genetically tractable archaeon *S. islandicus* is a model organism for studying virus-host dynamics in part because it encodes active CRISPR-Cas immunity, which can provide a historical record of virus-microbe interaction dynamics at a local scale.[13–15] CRISPR-Cas immunity utilizes a specific sequence match between a viral genome at a region called a protospacer and at least one spacer from a spacer array in the host resulting in protection of that cell from infection by the targeted virus. Previous studies of *S. islandicus* CRISPR arrays suggest an ongoing interaction between this species and the lytic S.

islandicus Rod-shaped Virus (SIRV).[16–18] Signatures in the structure of immune networks demonstrate that CRISPR immunity plays a strong role in shaping *S. islandicus* and viral diversity in nature. [19,20] Since *S. islandicus* is not the dominant species in hot springs, metagenomics is not able to efficiently uncover strain-level diversity of this host or its viruses to explore how CRISPR shapes virus-host interactions in this model system. Enzymatic amplification procedures such as multi-displacement amplification or rolling circle amplification can significantly increase genomic content before metagenomic sequencing, but these approaches struggle to adequately enrich viral genomes uniformly, particularly for linear genomes like that of SIRV.[21,22] Nonuniform enrichment can cause low-abundance individuals to drop out, and the resulting assemblies are often fragmentary or even chimeric.[23–25] Enrichment-based metagenomics can obtain a high yield of specific viruses by selecting a suitable bait host and growth media.[26] However, significant viral diversity is lost during enrichment as viral strains compete for resources, and small differences in fitness or growth rate can compound into large differences in abundance after enrichment.[27,28] Here, we demonstrate a straightforward digital enrichment of a diverse but relatively rare virus in a highly parallelized manner (Figure 1A). Since each virus is contained in its own unique droplet and the host is engineered to be CRISPR-deficient, we can eliminate immune selection and inter-strain competition to preserve natural variation during enrichment of a viral population. We demonstrate that (i) single virus enrichment in drops recovers greater viral diversity with the same sequencing power. In our model system, we show that this greatly increases the capacity to understand co-evolutionary dynamics by (ii) capturing those SIRV variants that would be lost due to strain competition during enrichment, and (iii) revealing the CRISPR-Cas mediated interactions that drive the local patterns of diversification in SIRV populations.

Results:

Drop Cultivation of Archaeal Viruses:

We developed a single-virus droplet culture system that isolates and provides a fixed pool of host resources and growth media to each individual virus strain from a complex environmental sample, constraining the differences in replication between diverse viruses. A thorough discussion of the development and optimization of archaeal growth in droplets is contained in the supplementary text. Briefly, we found that individual *S. islandicus* cells could be successfully

cultivated in >0.5 nL droplets, achieving an approximate 10-hour doubling time (Figure S1), which is comparable to the 8-hour doubling observed in liquid culture.[29] When growing viruses, we inoculated the growth media with a density of hosts and introduce dilute viruses through a second aqueous inlet, as shown in Figure 1B. This configuration ensures that viral attachment cannot occur before drop formation so that cells and viruses are loaded independently following a Poisson distribution.[30,31] To establish a naïve strain as our bait host, we selected an *S. islandicus* strain (RJW004) from a Kamchatka population where SIRVs have not been isolated and knocked out the *cas6* gene, which is essential to CRISPR-immune function.[32,33]

We used this host (RJW004Δ*cas6*) to isolate SIRV-NG34-Y22 (Figure 1C) and to validate single archaeal virus enrichment in drops, as shown in Figure 1D. The resulting linear relationship between the input and output viral titer is characteristic of a digital droplet loading, where each single virus drop yielded on average 92-fold ± (11) enrichment from a single SIRV. Since the enrichment process returns a viral stock with an increased titer, it can be used iteratively to reach the desired yield for sequencing, while facilitating competition-free expansion of a viral population.

Comparison of Drop and Bulk Enrichments using Environmental SIRVs:

To assess the effect of isolation in drops on viral diversity, we enriched SIRVs from an environmental sample in parallel using a bulk liquid culture and single virus drops until the minimum yield for PCR-free library prep was reached (~10^9 SIRV plaque-forming units (PFUs) per sample). Viral DNA was extracted, and each enriched metagenome was sequenced on Illumina and normalized to the same read depth. This workflow, summarized in Figure 2A, was applied to a direct viral concentrate as well as to the supernatant of a primary host culture from the same hot springs site. Figure 2B, C shows representative TEM images of the variety of virus-like particle morphologies we observed in the original concentrated sample, including the rod-shaped virions of SIRV. Following selective enrichment on the *S. islandicus* bait-host, SIRV-like particles became abundant in each sample (Figure 2D). Sequence analysis confirmed that each enriched metagenome yielded almost entirely SIRV genomic reads.

After quality filtering and read normalization, each metagenome was assembled de novo. The assembled contigs were retained if they contained a BLAST hits to any known SIRV genome. Reads were then mapped back to the filtered assembly to confirm that each enrichment

yielded primarily (>96%) SIRV-containing reads. In the absence of strain-level diversity, we would expect SIRV reads to construct a single contig at the average genome size of SIRV (32-36 kb). Increasing SIRV diversity and structural variants may cause breaks in the assembly corresponding to an increase in the total length of all contigs. Figure S2A shows the assembly metrics for each metagenome. Drop enrichments yielded greater assembly sizes than the corresponding bulk enrichments, although the differences are minor given the consistency of SIRV genomic architecture. Additionally, the contigs obtained from drop enrichment captured a larger share of the SIRV variable genome than the equivalent assembled bulk enrichment (Supplementary Table 1).

To explore the local diversity of SIRVs within this hot spring community, we used a reference-guided approach to identify individual variant loci.[34] By mapping reads to previously reported Yellowstone SIRVs, we determined that the genome of our new viral isolate from the same location (SIRV-Y22-NG34) provided the best reference, showing >99% covered bases and the highest fraction of reads mapping (>85%) (Figure S2B-C). Variant loci were identified using the Breseq pipeline in polymorphic mode with a threshold at 5% of coverage for each variant.[35] Given the substantial sequencing depth for each metagenome, coverage is >250× even for the rarest variants called. Figure 3A shows that more variants of all types (including small indels and junction candidates), as well as SNPs, were recovered when viral enrichment was performed in drops. As shown in Figure 3B-C, drop variants were more often multi-allelic, while bulk enrichment showed a greater proportion of fixed alleles. Figure 3C shows this distribution of SIRV variants across allele frequency and genome position. Drop enriched variants show a broad distribution of frequencies, while the bulk enrichment has largely collapsed to a handful of variants. Similarly, the variants identified from the direct drop enrichment display wider coverage across the genome than those sites identified from the direct bulk enrichment. These results are consistent with our expectation that single virus enrichment reduces or eliminates competition between strains, allowing more unique variants to persist above the detection threshold when sequenced. Analysis of the enrichments on the primary culture supernatant shows the same relationships between drop and bulk methods (Figure S3), demonstrating the repeatable effects of single virus encapsulation during enrichment. These results emphasize the utility of drop compartmentalization during enrichment, to maintain lower abundance strains and minor variants throughout an increase in viral titer of over 5 orders of magnitude.

Analysis of Local SIRV Diversification:

Next, we leveraged the SIRV variants recovered from each enrichment to understand the selective forces driving SIRV diversification within a single hot spring. The genome of SIRV-Y22-NG34 and its 45 open reading frames (ORFs) are shown in Figure 4A. Genes with known functions are labeled.[18,36–38] We first assessed if there were differences in variant accumulation among ORFs by calculating the length normalized number of variants per gene. Although there is significant variability (Figure 4C), the genes are distributed around the mean without any outliers. We next examined these types of variants to look for evidence of selection. SNPs that occur within an ORF were classified as synonymous or nonsynonymous. The direct drop enrichment captured sufficient variant coverage to compute the non-synonymous to synonymous rate ratio (dN/dS) across all but 5 genes (Figure 4B), while the equivalent bulk enrichment lacked sufficient data for 13 genes (Supplementary Table 2). Consistent with previous analyses of SIRV isolate genomes, we find low dN/dS values across most of the protein-coding portions of the genome, typical of purifying selection and genome maintenance.[18,36] The top hits showing increased dN/dS values were gp40 and gp43, both of which are a part of the SIRV accessory genome exclusive to Yellowstone.[36] These genes lack known functions but are positioned at the terminal ends of the genome, which has been identified as a focal site of variation among SIRV isolates.[36,39]

We compared the set of variants obtained from drop and bulk to identify those genomic regions that were differentially enriched during high between-strain competition in bulk culture. Figure 4B shows the difference in variants between enrichment types per bin across the genome, while Figure 4E and Supplementary Table 3 show the difference in variants between enrichment types per gene. This analysis identifies SIRV sites of variation in a natural population that are readily lost during inter-strain competition on a specific but were retained through drop compartmentalization. Interestingly, many of the multi-allelic variant sites in gp40 from the drop samples had become fixed in the bulk samples, which suggests that this gene plays an important role in competition for hosts; however, more work is needed to resolve any specific mechanism.

SIRV populations diversify in response to CRISPR selection

The CRISPR-Cas adaptive immune system recognizes and eliminates viral infections through a sequence match between the crRNA encoded by a spacer in the host and a protospacer in the virus. *S. islandicus* hosts feature multiple CRISPR-Cas systems, but Type I-A is the most abundant among sequenced isolates.[15] In vitro characterization of Type I-A CRISPR-Cas machinery has shown that a 5' protospacer adjacent motif (PAM) is needed in addition to a matched protospacer in order to target cleavage of the viral genome (Figure 5A).[40–42] The CCN motif has been established as the Type I-A PAM in *Sulfolobus*.[43–45] In addition to the requirement of an exact PAM, mismatches in the first eight nucleotides of the spacer-protospacer match, termed the seed region, contribute more strongly to immune evasion.[45–47] If CRISPR immunity plays a strong selective role in this natural population, we would expect that SIRV populations would accumulate escape mutations either in the PAM or in the matched protospacer, particularly within the seed region.

We used a previously reported set of *S. islandicus* host spacers obtained from a nearby hot springs community in Nymph Lake.[15] Since these hosts were sampled from a different site, protospacer matches to the virus (Figure 5B) likely reflect a shared ancestry or local resampling of protospacer sites. When the stringency of the spacer-protospacer matching criteria is increased, the Type I-A PAM emerges as the dominant 5' motif (Figure 5C), consistent with its role in spacer acquisition.[48,49] Figure 5D shows the enrichment of variants among the NG34 SIRV population within each CRISPR-targeted region. The accumulation of escape variants mirrors the *in vitro* potency of each type of escape mutation; the greatest enrichment is for PAM escapes, followed by mutations in the seed region, then the full protospacer, confirming the active role of CRISPR selection on a natural SIRV population.

To complement this spacer-matching analysis, we also analyzed the effects of CRISPR targeting without specific spacer sequences, by considering all possible PAM sequences of the form (XXN).[45] Each PAM divides the viral genome into two parts, so any position is either inside or outside the set of all possible protospacers defined by that sequence. We then compute the variant enrichment for each set of hypothetical protospacers (Figure 5B). Again, the CCN PAM emerges as the only motif showing significant enrichment for escapes across both the seed and protospacer regions. When the same analysis is performed using only the set of variants identified from bulk enrichment, the significance of the result is substantially reduced (Figure S5B). This highlights the importance of deep viral diversity facilitated by the drop enrichment to

the study of virus-host interactions through CRISPR-Cas systems in microbial populations, and that, given sufficient viral diversity, the evolutionary pressures applied to the virus by host spacers can be resolved without host sequences.

Conclusions and Perspectives:

We extended droplet culture methods to include hyperthermophilic archaea and their viruses, achieving highly parallelized enrichment of natural diversity. This approach is broadly applicable to natural populations of microbes and the viruses that infect them. Our results confirmed that the removal of competition between strains during enrichment dramatically improved the recovery of local variants without increasing sequencing costs. This straightforward approach to obtain drop-enriched metagenomes yielded over two thousand unique SNP variants, significantly expanding what is known about SIRV diversity, particularly revealing the extent of co-existing variants at the population level within a single hot springs site.

Along the same lines, drop compartmentalization can also be applied to explore the within-hot-springs diversity of archaeal host populations. By partitioning individual host cells for enrichment, large numbers of unique individuals can be expanded prior to sequencing or isolation. Likewise, modifying the chosen bait host can facilitate the selective enrichment of other archaeal viruses. Combining deep sampling of hosts and viruses enabled by enrichment in drops over time may provide new insights into viral host interactions and how they change within hot springs communities.

Sequences recovered within drop-enriched viral populations showed the effects of purifying selection across most of the SIRV genome and signals of relaxed selection within portions of the accessory genome. By comparing the patterns of variation between drop and bulk enrichment, we had the unique opportunity to observe both the high fitness alleles that became fixed in the population during competition in the bulk enrichments and the lower fitness alleles that were maintained only when strain competition was removed. These sites may provide a signature of host-specific adaptation as those alleles show differential fitness on the single genotype bait-host used during enrichment. We further leveraged the local SIRV diversity to explore CRISPR-immune selection on the viral genome, where viral-host interactions are mediated through the Type I-A defense system. We resolved the signature of viral escape mutations, highlighting the active role of CRISPR-immunity in SIRV populations. Deep

sampling microbial viruses enabled by enrichment in drops over time will provide new insights into the dynamics of viral-host interactions and how they change within microbial communities.

Experimental Methods:

Characterization and Quantification of Cells and Viruses:

A Δ*cas6* mutant was constructed in the RJW004 strain background, which is derived from the wild-type *S. islandicus* M.16.4 isolated from a hot spring in Kamchatka, using a plasmid integration and segregation knockout strategy as previously described.[32] This mutant is deficient in crRNA processing and, therefore, is unable to mount an adaptive CRISPR immune response.[33] This host is broadly susceptible to SIRVs, including the majority of Yellowstone SIRVs,[36] while being genetically tractable. *S. islandicus* strains were routinely cultivated in 1× DT (pH 3.5), composed of basal salts, trace minerals, 0.1% (w/v) dextrin, and 0.1% (w/v) EZMix-N-Z-amine A.[50] For the growth of auxotrophic strain RJW004 and its derivatives, the medium was further supplemented with 20 µg/mL uracil (U) and 50 µg/mL agmatine (A).

Quantification of virus titers was performed by spotting dilutions of the virus on a lawn of hosts and monitoring the formation of plaques within 7 days. After determining an appropriate viral dilution factor by spot-on-lawn assay, accurate quantification was performed as follows. Approximately 3×10^8 host cells were spun down and resuspended in 500 µL fresh DTUA media. To this, 100 µL of diluted virus was added and mixed well prior to overlay plating.[51] After 5-7 days, plaques were enumerated and averaged across three replicate plates.

Routine cell growth was monitored by OD_{600} measurements with a CO8000 cell density meter (WPA, Cambridge, United Kingdom). For precise cell enumeration, flow cytometry was used as follows: Cell samples were diluted 10-fold into fresh media and injected into a BD Symphony A1 cell analyzer and compared against cell-free media. Cells were gated using Forward scatter (FSC) and side scatter (SSC). Each sample is measured three times for 2 minutes and averaged to obtain the cell concentration. The resulting linear relationship between cell-gated events and OD_{600} enables quantification even of very dilute samples (below OD_{600} 0.02) with minimal sample loss (50 µL total for measurement).

Electron Microscopy:

TEM grids were prepared using ~10 µL of viral sample and negatively stained with 2% (wt/vol) uranyl acetate prior to imaging using a FEI Tecnai G2 F20 S-TWIN STEM (Thermo-fisher) operated at 120 kV, as previously described.[52]

Encapsulation and Recovery of *S. islandicus* from Culture Drops:

Droplet generation devices were fabricated using conventional soft-lithography techniques to imprint channels in PDMS using a device master mold prepared by exposing and developing SU-8 negative photoresist (Kayaku). Device ports were added using a biopsy punch and then bonded to glass slides to complete the device. To ensure proper wetting, a fluorophilic coating was applied to the channel surfaces using Aquapel. The device design features two aqueous inlets and one oil inlet that meet at a flow-focusing junction. When operating in the dripping regime, highly monodisperse droplets could be generated in the range of ~50 pL to 5 nL. An example of typical SIRV cultivation, aq1 + aq2 = 500 µL/h, while the oil phase consists of 2% w/w RAN in HFE at 50 µL/h. Droplets are collected off chip and transferred to a 96-well plate. We found that the droplet culture could remain sufficiently oxygenated and stable in size when ~220 µL of uncovered droplets were added to each well. The addition of 10 µL 5% w/w RAN in HFE supplemented the surfactant used during drop making and successfully stabilized the emulsion throughout long-term incubation at 76 °C, the optimal growth temperature of *S. islandicus*. Quantitative recovery of cells/viruses following cultivation in drops was achieved using an electrostatic coalescence. The usual approach to drop recovery uses a chemical de-emulsifier such as 20% PFO or 5% PFB. However, this treatment resulted in a significant loss of cell viability (supplemental data) and infectious titers for enveloped viruses. Instead, the emulsion was rotated at the tip of an SPI Westek workstation deionizer until a clear aqueous layer could be seen on top of the oil. The recovered aqueous phase was carefully transferred to a clean tube. We confirmed successful quantitative recovery of the host and virus with this approach.

Droplet cultivation conditions for *S. islandicus and* SIRV:

To grow single archaea cells in drops, cell/virus suspensions in *Saccharolobus* media are injected into the device using syringe pumps. The continuous phase consists of 2 wt% 008-fluorsurfactant (RAN) in Novec-7500 (3M). The flow rates of the oil and aqueous phases were

tuned to produce ~0.5-1 nL droplets that were collected off-chip. Droplets are carefully transferred to a flat-bottom 96-well plate. Approximately 250 µL of emulsion drops are added to each well and then surrounded by 250 µL of media in each adjacent well. The plate is then sealed with foil, wrapped in a damp cloth, and stacked among blank plates in three bags (Ziploc), prior to transfer to a pre-heated incubator held at 76 °C. To recover live/viable cells from drops necessitated electrostatic de-emulsification. After dilution of the surfactant by oil removal and rinsing, the emulsion was gently rotated at the tip of a workstation ionizer (SPIWestek) until fully coalesced. Use of chemical de-emulsifiers resulted in significant cell death.

Enrichment of single viruses using host cell-filled droplets: To ensure that cells and viruses follow a Poisson loading during drop formation, a dropmaker with two aqueous inlets is used to ensure that cells and viruses remain separated prior to compartmentalization. The two aqueous phases meet during drop generation and co-flow without mixing prior to resulting in an average of 10 cells, less than 0.1 viruses, and 1X DT media after the cell stream and virus stream are mixed 4:1 in accordance with their flow rates (400:100 µL hr^{-1}). The oil phase was used to control the drop size to be ~1 nL (100 µL hr^{-1}). As before, drops were transferred to 96-well plates for long-term incubation. Virus concentrations were measured by plaque counting.

Hot springs sampling and enrichment cultures:

Hot springs samples were collected from the Norris Geyser Basin of Yellowstone National Park, United States, in October of 2022 and in 2023 (44°43'46.3"N 110°42'43.2"W). The temperature and pH were measured to be 62.4 °C and 4.29 in 2022 and 62.9 °C and 4.63 in 2023, confirming this site has maintained suitable growth conditions for *Saccharolobus*.

For the direct sample, we collected 20 L of hot spring water, including mud and sediment, which was collected and processed as follows. Large sediment was allowed to settle, and the supernatant was decanted through a 0.45 µM bottle-top filter. After filtration, the volume was reduced by ~10,000× using Spin-X concentrators (100 Kda cutoff) to yield ~2 mL of direct viral concentrate. 10 µL each was used for screening by TEM and PFU quantification on the RJW004Δ*cas6* host. The remaining virus concentrate was divided equally and enriched in drops and in bulk.

For the primary culture, an additional 2 L of hot spring water was collected at the same time to inoculate cultures and for routine sampling. For a total of 10 flasks prepared and grown

in parallel, 5 mL of sample was added to 95 mL of DT media and incubated at 76 °C for 10 days. After incubation, these flasks were pooled and combined to yield the ~1 L primary culture, which was centrifuged at 3,900 rpm for 30 minutes, and the supernatant was filtered through a 0.22 μm membrane to obtain the viral fraction. Viral particles were visualized by TEM and quantified by a plaque assay. The sample was then divided in half and enriched in drops or in bulk until the total PFU of the sample reached ~10^9.

DNA extraction, library preparation, and Sequencing:

Viruses were concentrated using a Beckman Optima LE-80K ultracentrifuge equipped with SW-55 Ti swing-bucket rotor at 40,000 rpm for 5 hours at 10 °C. The viral pellet was resuspended in 100 μL of 1× DT medium and treated with DNase I and RNase I at 37 °C for 2 hours to degrade contaminating nucleic acids. Viral genomic DNA was then extracted following the protocol described previously.[53] DNA was quantified with a Qubit fluorometer, and samples with >50 ng DNA were used for Illumina library preparation kit (Tecan) and pooled for sequencing on a Novaseq X with V1.0 reagents (paired-end; 2 × 150 bp). Fastq files were generated and demultiplexed with the bcl2fastq v2.20 Conversion Software (Illumina). Reads were quality filtered and trimmed with Trimmomatic and subsampled to 25 million paired reads per sample with seqtoolkit.

Bioinformatic analysis of SIRV Sequences:

The trimmed and quality-filtered SIRV metagenomic reads were aligned using minimap2, and the resulting alignments were analyzed using samtools. SIRV isolate reads were assembled using SPAdes with default parameters. The resulting GFA was examined in Bandage to resolve the inverted terminal repeats and obtain a closed SIRV genome, which was also used for alignment of SIRV metagenomes. Genome annotation was performed using Prokka and curated using blastp. Each viral population was assembled using SPAdes in metaviral mode. To identify variant loci, we ran Breseq in polymorphism mode on the trimmed and quality-controlled reads with a SNP cutoff at 0.5% of read coverage across the site. CRISPR analysis was performed using cctk and blastn short to identify each possible protospacer adjacent motif alignment to the SIRV genome.[54] These alignments were processed using a custom Python script to count variant positions that overlap the identified seed and spacer regions.

Data Availability:

All raw sequence files and the assembled SIRV isolate genome used in this work are deposited with NCBI under Bioproject PRJNA1310652.

Author Contributions:

T.C., C.Z., H.-S.H., and R.W. conceived the study, with advice and support from M.Y. Environmental sampling was performed by T.C, C.Z., and J.Y. Archaeal cell and virus droplet experiments were developed by T.C and C.-L.C, assisted by C.Z. and J.Y. Flow cytometry was performed by T.C and J.Y. C.Z. carried out virus screening, isolation, quantification, imaging, purification, characterization, and sequencing, and contributed to the development of the host-virus baiting system using CRISPR-deficient mutants for targeted virus enrichment. Bioinformatics and data analysis were conducted by T.C with advice from C.Z., H.-S.H., and R.W. Writing was led by T.C and C.Z. with revisions from H.-S.H. and R.W. All authors read and approved the final paper.

Acknowledgements:

We thank Catherine L. Wallace and T Josek at the Beckman Institute for Advanced Science & Technology, UIUC, for their assistance with TEM. We would like to thank the Roy J. Carver Biotechnology Center for their support in sequencing and library preparation. We also thank the Gordon and Betty Moore Foundation through Grant GBMF9195 to Rachel J. Whitaker. Environmental samples were collected under Yellowstone National Park permit number 5684.

Figures:

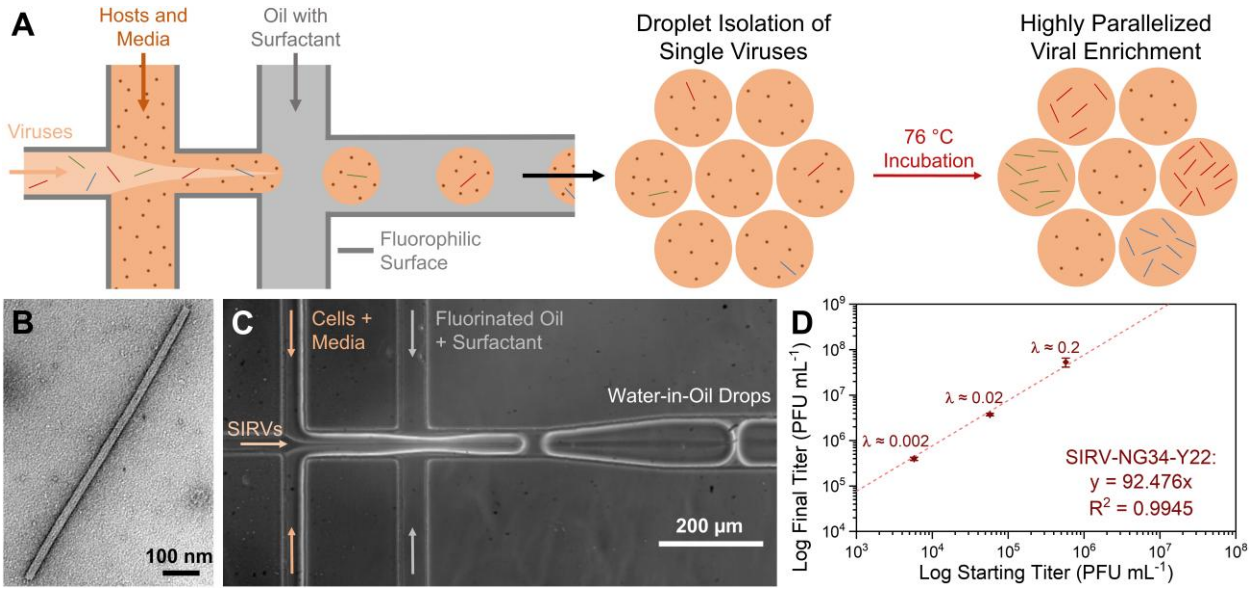


Figure 1: A) Schematic representation of single archaeal virus cultivation in drops. Viruses and hosts are separated across two aqueous inlets, which ensures that each is encapsulated following a Poisson random loading. Since each occupied compartment contains a limited number of bait hosts and a single virus, replication at each stage is constrained, ensuring uniformity across diverse strains. B) Microfluidic drop generation for enrichment of individual archaeal viruses. D) TEM image of SIRV-NG34-Y22. E) Quantification of SIRV enrichment in drops.

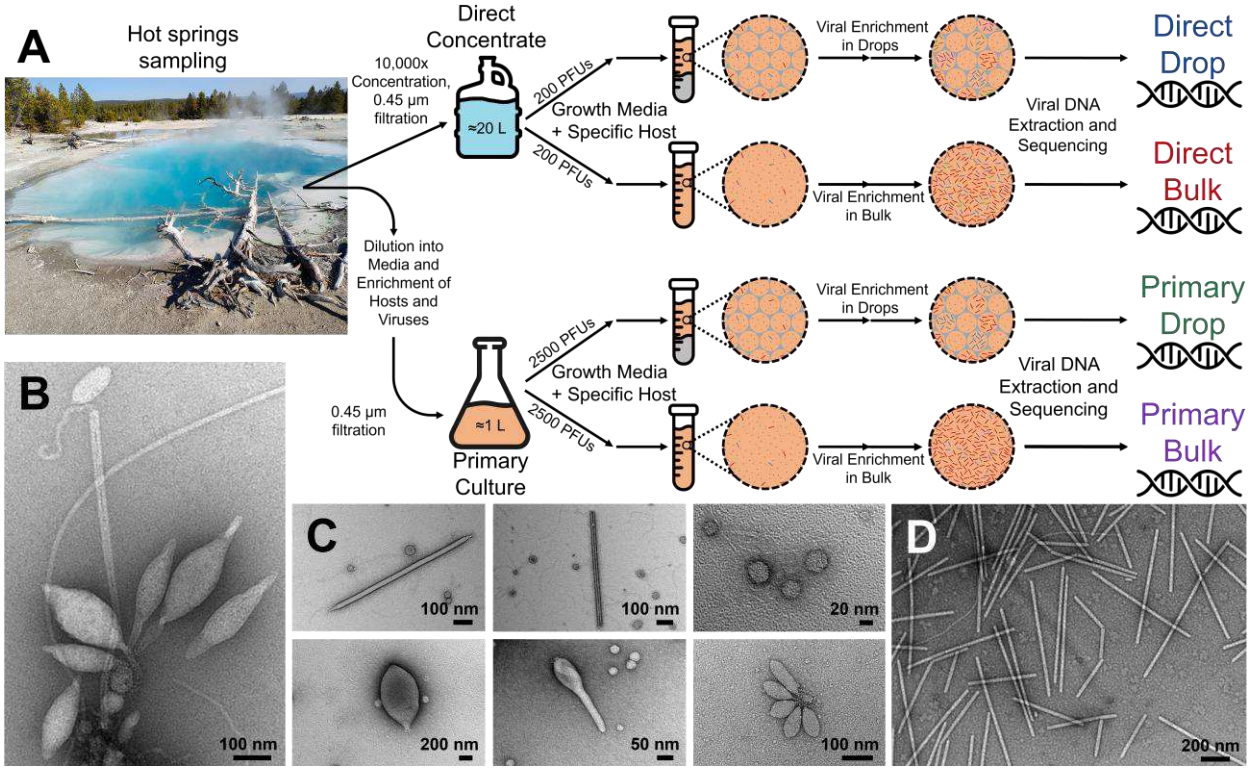


Figure 2: A) Sampling scheme for SIRV-enriched metagenomes from a hot springs site in the Norris Geyser Basin. For direct sampling, 20 L of hot spring water and sediment were filtered and concentrated down to 2 mL. For primary culture, ~1 L of viral supernatant was

collected after growing local hosts and viruses in *Saccharolobus* growth media. Samples were then enriched in parallel using either liquid culture (bulk) or isolated into drops for single virus enrichment (drop). Inset TEM image of the supernatant of the primary culture showing a variety of virus-like particle morphologies, including SIRV-like particles. After enrichment, viral genomic DNA was extracted and sequenced to obtain metagenomes for each population. B) Example TEM images from (B) the supernatant of the primary culture and (C) the direct viral concentrate from NG34. Virus-like particles with diverse morphologies, including SIRV-like particles, can be observed. D) Representative TEM image after enrichment. SIRV-like particles become abundant after enrichment on *S. islandicus* RJW004.

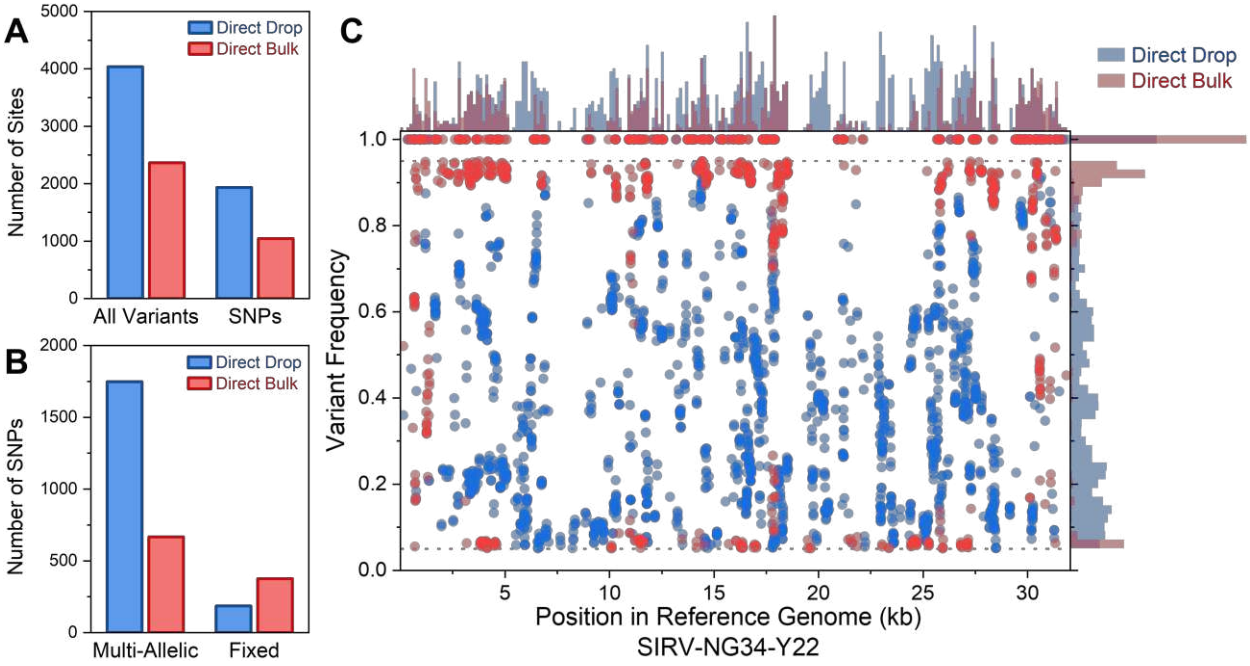


Figure 3: Comparison of SIRV variants identified from bulk and drop enrichments of the direct sample. A) Total number of variant sites. All variants, including SNPs, single-base insertions and deletions, larger indels, and junction candidates. B) Total number of SNPs (including single base indels) that are fixed in the population or multi-allelic above the threshold of 5%. C) Distribution of variants plotted across the SIRV reference genome and across frequency in the metagenome. The variants identified from the drop enrichment are distributed more broadly across the genome. The drop enrichment also preserved more minor variants, resulting in more total SNPs, including more multi-allelic sites.

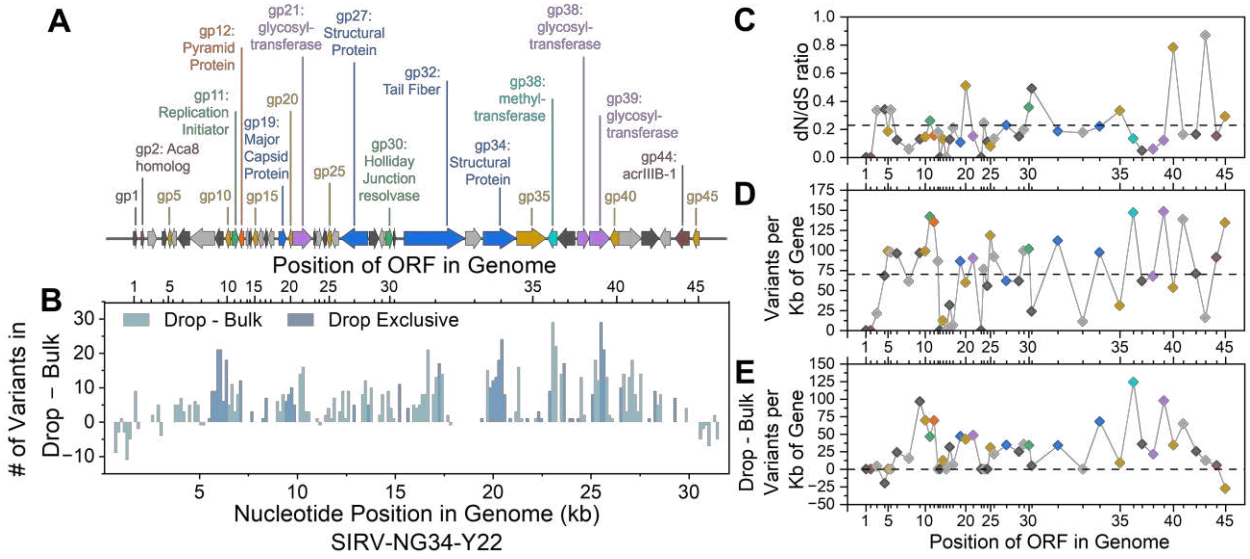


Figure 4: Per gene analysis of SIRV variation. A) Annotated reference genome of SIRV-Y22-NG34. B) The number of identified SIRV variants from drop enrichment minus those from bulk enrichment within ~150 bp bins. Those bins where no variants were identified in bulk are highlighted as drop exclusive. C) Analysis of the dN/dS ratio for all genes. Elevated values indicate the effects of positive selection, while low values signify the effects of purifying selection. D) Comparison of variant frequency across genes. Each value is normalized by length to 1 kb. Genes with higher rates of variation. E) Analysis of SIRV genes that displayed higher rates of variation in the direct drop enrichment relative to the direct bulk enrichment, normalized by length to 1kb.

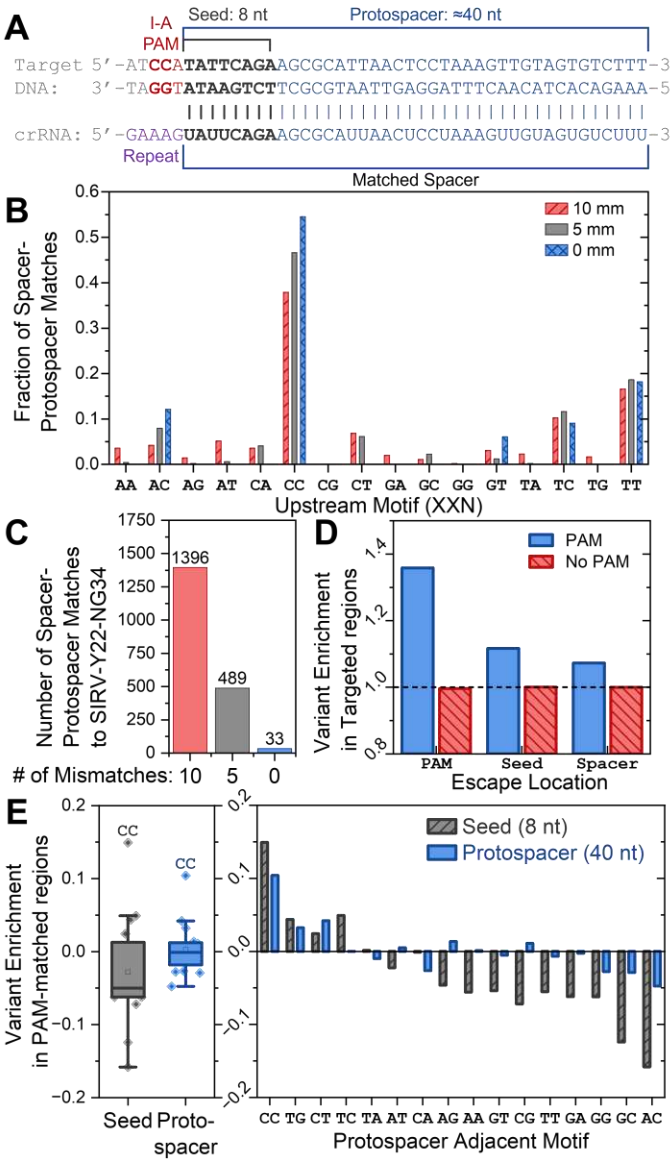


Figure 5: Analysis of CRISPR targeting dynamics on local SIRV diversification. A) Schematic illustrating the key components of a CRISPR targeting interaction between SIRV and the type I-A system of *S. islandicus*. The processed crRNA can anneal to a matching portion of the viral genome, initiating cleavage of the DNA. B-C) Identification of upstream dinucleotide motifs using YNP host spacers matching SIRV with 10, 5, or 0 allowed mismatches. The Type I-A motif is the dominant PAM. D) SIRV variants are enriched in regions targeted by active spacers in the host immune repertoire. Results of hypothetical protospacer match analysis against XXA motifs. The characteristic CCN motif of the Type I-A CRISPR system of *S. islandicus* shows clear enrichment in the downstream protospacer region.

References:

(1) Prangishvili, D. The Wonderful World of Archaeal Viruses. *Annu. Rev. Microbiol.* **2013**, *67* (Volume 67, 2013), 565–585. https://doi.org/10.1146/ANNUREV-MICRO-092412-155633/CITE/REFWORKS.

(2) Manrique, P.; Bolduc, B.; Walk, S. T.; van der Oost, J.; de Vos, W. M.; Young, M. J. Healthy Human Gut Phageome. *Proc. Natl. Acad. Sci. U. S. A.* **2016**, *113* (37), 10400–10405. https://doi.org/10.1073/pnas.1601060113.
(3) Chevallereau, A.; Pons, B. J.; van Houte, S.; Westra, E. R. Interactions between Bacterial and Phage Communities in Natural Environments. *Nature Reviews Microbiology 2021 20:1* **2021**, *20* (1), 49–62. https://doi.org/10.1038/s41579-021-00602-y.
(4) Suttle, C. A. Marine Viruses — Major Players in the Global Ecosystem. *Nat. Rev. Microbiol.* **2007**, *5* (10), 801–812. https://doi.org/10.1038/nrmicro1750.
(5) DeWerff, S. J.; Bautista, M. A.; Pauly, M.; Zhang, C.; Whitaker, R. J. Killer Archaea: Virus-Mediated Antagonism to CRISPR-Immune Populations Results in Emergent Virus-Host Mutualism. *mBio* **2020**, *11* (2). https://doi.org/10.1128/mBio.00404-20.
(6) Chen, J.; Novick, R. P. Phage-Mediated Intergeneric Transfer of Toxin Genes. *Science (1979).* **2009**, *323* (5910), 139–141. https://doi.org/10.1126/SCIENCE.1164783;WEBSITE:WEBSITE:AAAS-SITE;JOURNAL:JOURNAL:SCIENCE;WGROUP:STRING:PUBLICATION.
(7) Brito, I. L. Examining Horizontal Gene Transfer in Microbial Communities. *Nature Reviews Microbiology 2021 19:7* **2021**, *19* (7), 442–453. https://doi.org/10.1038/s41579-021-00534-7.
(8) Vetsigian, K. Diverse Modes of Eco-Evolutionary Dynamics in Communities of Antibiotic-Producing Microorganisms. *Nature Ecology & Evolution 2017 1:7* **2017**, *1* (7), 0189-. https://doi.org/10.1038/s41559-017-0189.
(9) Pilosof, S.; Alcalá-Corona, S. A.; Wang, T.; Kim, T.; Maslov, S.; Whitaker, R.; Pascual, M. The Network Structure and Eco-Evolutionary Dynamics of CRISPR-Induced Immune Diversification. *Nat. Ecol. Evol.* **2020**, *4* (12), 1650–1660. https://doi.org/10.1038/s41559-020-01312-z.
(10) Whitaker, R. J.; Grogan, D. W.; Taylor, J. W. Geographic Barriers Isolate Endemic Populations of Hyperthermophilic Archaea. *Science (1979).* **2003**, *301* (5635), 976–978. https://doi.org/10.1126/science.1086909.
(11) Siering, P. L.; Clarke, J. M.; Wilson, M. S. Geochemical and Biological Diversity of Acidic, Hot Springs in Lassen Volcanic National Park. *Geomicrobiol. J.* **2006**, *23* (2), 129–141. https://doi.org/10.1080/01490450500533916.
(12) Held, N. L.; Whitaker, R. J. Viral Biogeography Revealed by Signatures in Sulfolobus Islandicus Genomes. *Environ. Microbiol.* **2009**, *11* (2), 457–466. https://doi.org/10.1111/j.1462-2920.2008.01784.x.
(13) Held, N. L.; Herrera, A.; Quiroz, H. C.; Whitaker, R. J. CRISPR Associated Diversity within a Population of Sulfolobus Islandicus. *PLoS One* **2010**, *5* (9), e12988. https://doi.org/10.1371/journal.pone.0012988.
(14) Bautista, M. A.; Zhang, C.; Whitaker, R. J. Virus-Induced Dormancy in the Archaeon Sulfolobus Islandicus. *mBio* **2015**, *6* (2). https://doi.org/10.1128/mBio.02565-14.
(15) Pauly, M. D.; Bautista, M. A.; Black, J. A.; Whitaker, R. J. Diversified Local CRISPR-Cas Immunity to Viruses of Sulfolobus Islandicus. *Philos. Trans. R. Soc. Lond. B Biol. Sci.* **2019**, *374* (1772), 20180093. https://doi.org/10.1098/rstb.2018.0093.
(16) Karginov, F. V.; Hannon, G. J. The CRISPR System: Small RNA-Guided Defense in Bacteria and Archaea. *Mol. Cell* **2010**, *37* (1), 7–19. https://doi.org/10.1016/J.MOLCEL.2009.12.033/ASSET/B1CFB3CE-D3CD-457D-9AA4-8132D43B0FFC/MAIN.ASSETS/GR5.JPG.

(17) Koonin, E. V.; Makarova, K. S.; Wolf, Y. I. Evolutionary Genomics of Defense Systems in Archaea and Bacteria. *Annu. Rev. Microbiol.* **2017**, *71* (Volume 71, 2017), 233–261. https://doi.org/10.1146/ANNUREV-MICRO-090816-093830/CITE/REFWORKS.
(18) Fackler, J. R.; Dworjan, M.; Gazi, K. S.; Grogan, D. W. Diversity of SIRV-like Viruses from a North American Population. *Viruses* **2022**, *14* (7). https://doi.org/10.3390/V14071439/S1.
(19) Anderson, R. E.; Kouris, A.; Seward, C. H.; Campbell, K. M.; Whitaker, R. J. Structured Populations of Sulfolobus Acidocaldarius with Susceptibility to Mobile Genetic Elements. *Genome Biol. Evol.* **2017**, *9* (6), 1699–1710. https://doi.org/10.1093/GBE/EVX104.
(20) Campbell, K. M.; Kouris, A.; England, W.; Anderson, R. E.; McCleskey, R. B.; Nordstrom, D. K.; Whitaker, R. J. Sulfolobus Islandicus Meta-Populations in Yellowstone National Park Hot Springs. *Environ. Microbiol.* **2017**, *19* (6), 2334–2347. https://doi.org/10.1111/1462-2920.13728.
(21) Shoaib, M.; Baconnais, S.; Mechold, U.; Le Cam, E.; Lipinski, M.; Ogryzko, V. Multiple Displacement Amplification for Complex Mixtures of DNA Fragments. *BMC Genomics* **2008**, *9* (1), 1–14. https://doi.org/10.1186/1471-2164-9-415/FIGURES/5.
(22) Parras-Moltó, M.; Rodríguez-Galet, A.; Suárez-Rodríguez, P.; López-Bueno, A. Evaluation of Bias Induced by Viral Enrichment and Random Amplification Protocols in Metagenomic Surveys of Saliva DNA Viruses. *Microbiome 2018 6:1* **2018**, *6* (1), 1–18. https://doi.org/10.1186/S40168-018-0507-3.
(23) Marine, R.; McCarren, C.; Vorrasane, V.; Nasko, D.; Crowgey, E.; Polson, S. W.; Wommack, K. E. Caught in the Middle with Multiple Displacement Amplification: The Myth of Pooling for Avoiding Multiple Displacement Amplification Bias in a Metagenome. *Microbiome* **2014**, *2* (1), 3. https://doi.org/10.1186/2049-2618-2-3.
(24) Alneberg, J.; Karlsson, C. M. G.; Divne, A.-M.; Bergin, C.; Homa, F.; Lindh, M. V.; Hugerth, L. W.; Ettema, T. J. G.; Bertilsson, S.; Andersson, A. F.; Pinhassi, J. Genomes from Uncultivated Prokaryotes: A Comparison of Metagenome-Assembled and Single-Amplified Genomes. *Microbiome* **2018**, *6* (1), 173. https://doi.org/10.1186/s40168-018-0550-0.
(25) Dutilh, B. E.; Varsani, A.; Tong, Y.; Simmonds, P.; Sabanadzovic, S.; Rubino, L.; Roux, S.; Muñoz, A. R.; Lood, C.; Lefkowitz, E. J.; Kuhn, J. H.; Krupovic, M.; Edwards, R. A.; Brister, J. R.; Adriaenssens, E. M.; Sullivan, M. B. Perspective on Taxonomic Classification of Uncultivated Viruses. *Curr. Opin. Virol.* **2021**, *51*, 207–215. https://doi.org/10.1016/J.COVIRO.2021.10.011.
(26) Liu, Y.; Brandt, D.; Ishino, S.; Ishino, Y.; Koonin, E. V.; Kalinowski, J.; Krupovic, M.; Prangishvili, D. New Archaeal Viruses Discovered by Metagenomic Analysis of Viral Communities in Enrichment Cultures. *Environ. Microbiol.* **2019**, *21* (6), 2002–2014. https://doi.org/10.1111/1462-2920.14479.
(27) Dunbar, J.; White, S.; Forney, L. Genetic Diversity through the Looking Glass: Effect of Enrichment Bias. *Appl. Environ. Microbiol.* **1997**, *63* (4), 1326–1331. https://doi.org/10.1128/AEM.63.4.1326-1331.1997;PAGE:STRING:ARTICLE/CHAPTER.
(28) Diaz-Garcia, L.; Huang, S.; Sproer, C.; Sierra-Ramírez, R.; Bunk, B.; Overmann, J.; Jimenez, D. J.; Overmann, J. Dilution-to-Stimulation/Extinction Method: A Combination Enrichment Strategy To Develop a Minimal and Versatile Lignocellulolytic Bacterial

Consortium. *Appl. Environ. Microbiol.* **2020**, *87* (2), 1–15. https://doi.org/10.1128/AEM.02427-20/SUPPL_FILE/AEM.02427-20-S0001.PDF.
(29) Quehenberger, J.; Albersmeier, A.; Glatzel, H.; Hackl, M.; Kalinowski, J.; Spadiut, O. A Defined Cultivation Medium for Sulfolobus Acidocaldarius. *J. Biotechnol.* **2019**, *301*, 56–67. https://doi.org/10.1016/J.JBIOTEC.2019.04.028.
(30) Shah, R. K.; Shum, H. C.; Rowat, A. C.; Lee, D.; Agresti, J. J.; Utada, A. S.; Chu, L. Y.; Kim, J. W.; Fernandez-Nieves, A.; Martinez, C. J.; Weitz, D. A. Designer Emulsions Using Microfluidics. *Materials Today*. Elsevier April 1, 2008, pp 18–27. https://doi.org/10.1016/S1369-7021(08)70053-1.
(31) Abate, A. R.; Chen, C.-H.; Agresti, J. J.; Weitz, D. A. Beating Poisson Encapsulation Statistics Using Close-Packed Ordering. *Lab Chip* **2009**, *9* (18), 2628. https://doi.org/10.1039/b909386a.
(32) Zhang, C.; Cooper, T. E.; Krause, D. J.; Whitaker, R. J. Augmenting the Genetic Toolbox for Sulfolobus Islandicus with a Stringent Positive Selectable Marker for Agmatine Prototrophy. *Appl. Environ. Microbiol.* **2013**, *79* (18), 5539–5549. https://doi.org/10.1128/AEM.01608-13.
(33) Peng, W.; Li, H.; Hallstrøm, S.; Peng, N.; Liang, Y. X.; She, Q. Genetic Determinants of PAM-Dependent DNA Targeting and Pre-CrRNA Processing in Sulfolobus Islandicus. *RNA Biol.* **2013**, *10* (5), 738–748. https://doi.org/10.4161/RNA.23798/ASSET/D5AC0A73-5719-42E4-ACB6-2D2D6488E1CD/ASSETS/IMAGES/LARGE/KRNB_A_10923798_F0003.JPG.
(34) Olm, M. R.; Butterfield, C. N.; Copeland, A.; Boles, T. C.; Thomas, B. C.; Banfield, J. F. The Source and Evolutionary History of a Microbial Contaminant Identified through Soil Metagenomic Analysis. *mBio* **2017**, *8* (1). https://doi.org/10.1128/MBIO.01969-16/SUPPL_FILE/MBO001173203SD1.TXT.
(35) Deatherage, D. E.; Barrick, J. E. Identification of Mutations in Laboratory-Evolved Microbes from next-Generation Sequencing Data Using Breseq. *Methods in molecular biology* **2014**, *1151*, 165–188. https://doi.org/10.1007/978-1-4939-0554-6_12.
(36) Bautista, M. A.; Black, J. A.; Youngblut, N. D.; Whitaker, R. J. Differentiation and Structure in Sulfolobus Islandicus Rod-Shaped Virus Populations. *Viruses* **2017**, *9* (5), 120. https://doi.org/10.3390/v9050120.
(37) Quemin, E. R. J.; Lucas, S.; Daum, B.; Quax, T. E. F.; Kühlbrandt, W.; Forterre, P.; Albers, S.-V.; Prangishvili, D.; Krupovic, M. First Insights into the Entry Process of Hyperthermophilic Archaeal Viruses. *J. Virol.* **2013**, *87* (24), 13379–13385. https://doi.org/10.1128/jvi.02742-13.
(38) Bhoobalan-Chitty, Y.; Xu, S.; Martinez-Alvarez, L.; Karamycheva, S.; Makarova, K. S.; Koonin, E. V.; Peng, X. Regulatory Sequence-Based Discovery of Anti-Defense Genes in Archaeal Viruses. *Nature Communications 2024 15:1* **2024**, *15* (1), 3699-. https://doi.org/10.1038/s41467-024-48074-x.
(39) Bhoobalan-Chitty, Y.; Johansen, T. B.; Di Cianni, N.; Peng, X. Inhibition of Type III CRISPR-Cas Immunity by an Archaeal Virus-Encoded Anti-CRISPR Protein. *Cell* **2019**, *179* (2), 448-458.e11. https://doi.org/10.1016/J.CELL.2019.09.003.
(40) Hidalgo-Cantabrana, C.; Barrangou, R. Characterization and Applications of Type I CRISPR-Cas Systems. *Biochem. Soc. Trans.* **2020**, *48* (1), 15–23. https://doi.org/10.1042/BST20190119.

(41) Liu, T.; Xu, Y.; Wang, X.; Ye, Q.; Liu, Z.; Zhang, Z.; Liu, J.; Yang, Y.; Peng, X.; Peng, N. DNA Motifs and an Accessory CRISPR Factor Determine Cas1 Binding and Integration Activity in Sulfolobus Islandicus. *Int. J. Mol. Sci.* **2022**, *23* (17), 10178. https://doi.org/10.3390/IJMS231710178/S1.
(42) Sorek, R.; Lawrence, C. M.; Wiedenheft, B. CRISPR-Mediated Adaptive Immune Systems in Bacteria and Archaea. *Annu. Rev. Biochem.* **2013**, *82* (Volume 82, 2013), 237–266. https://doi.org/10.1146/annurev-biochem-072911-172315.
(43) Gudbergsdottir, S.; Deng, L.; Chen, Z.; Jensen, J. V. K.; Jensen, L. R.; She, Q.; Garrett, R. A. Dynamic Properties of the Sulfolobus CRISPR/Cas and CRISPR/Cmr Systems When Challenged with Vector-Borne Viral and Plasmid Genes and Protospacers. *Mol. Microbiol.* **2011**, *79* (1), 35–49. https://doi.org/10.1111/J.1365-2958.2010.07452.X.
(44) Zhao, P.; Bi, X.; Wang, X.; Feng, X.; Shen, Y.; Yuan, G.; She, Q. Rational Design of Unrestricted PRN1 Derivatives and Their Application in the Construction of a Dual Plasmid Vector System for Saccharolobus Islandicus. *mLife* **2024**, *3* (1), 119–128. https://doi.org/10.1002/MLF2.12107.
(45) Mousaei, M.; Deng, L.; She, Q.; Garrett, R. A. Major and Minor CrRNA Annealing Sites Facilitate Low Stringency DNA Protospacer Binding Prior to Type I-A CRISPR-Cas Interference in Sulfolobus. *RNA Biol.* **2016**, *13* (11), 1166–1173. https://doi.org/10.1080/15476286.2016.1229735.
(46) Manica, A.; Zebec, Z.; Steinkellner, J.; Schleper, C. Unexpectedly Broad Target Recognition of the CRISPR-Mediated Virus Defence System in the Archaeon Sulfolobus Solfataricus. *Nucleic Acids Res.* **2013**, *41* (22), 10509. https://doi.org/10.1093/NAR/GKT767.
(47) Li, Y.; Pan, S.; Zhang, Y.; Ren, M.; Feng, M.; Peng, N.; Chen, L.; Liang, Y. X.; She, Q. Harnessing Type I and Type III CRISPR-Cas Systems for Genome Editing. *Nucleic Acids Res.* **2015**, *44* (4), 34. https://doi.org/10.1093/nar/gkv1044.
(48) Erdmann, S.; Shah, S. A.; Garrett, R. A. SMV1 Virus-Induced CRISPR Spacer Acquisition from the Conjugative Plasmid PMGB1 in Sulfolobus Solfataricus P2. *Biochem. Soc. Trans.* **2013**, *41* (6), 1449–1458. https://doi.org/10.1042/BST20130196.
(49) Bhoobalan-Chitty, Y.; Duan, X.; Peng, X. High-MOI Induces Rapid CRISPR Spacer Acquisition in Sulfolobus from an Acr Deficient Virus. *MicroPubl. Biol.* **2022**, *2022*, 10.17912/micropub.biology.000664. https://doi.org/10.17912/micropub.biology.000664.
(50) Zhang, C.; Whitaker, R. J. Microhomology-Mediated High-Throughput Gene Inactivation Strategy for the Hyperthermophilic Crenarchaeon Sulfolobus Islandicus. *Appl. Environ. Microbiol.* **2018**, *84* (1), 2167–2184. https://doi.org/10.1128/AEM.02167-17.
(51) Redder, P.; Peng, X.; Brügger, K.; Shah, S. A.; Roesch, F.; Greve, B.; She, Q.; Schleper, C.; Forterre, P.; Garrett, R. A.; Prangishvili, D. Four Newly Isolated Fuselloviruses from Extreme Geothermal Environments Reveal Unusual Morphologies and a Possible Interviral Recombination Mechanism. *Environ. Microbiol.* **2009**, *11* (11), 2849–2862. https://doi.org/10.1111/J.1462-2920.2009.02009.X.
(52) Zhang, C.; Wipfler, R. L.; Li, Y.; Wang, Z.; Hallett, E. N.; Whitaker, R. J. Cell Structure Changes in the Hyperthermophilic Crenarchaeon Sulfolobus Islandicus Lacking the S-Layer. *mBio* **2019**, *10* (4). https://doi.org/10.1128/mBio.01589-19.
(53) Zhang, J.; Zheng, X.; Wang, H.; Jiang, H.; Dong, H.; Huang, L. Novel Sulfolobus Fuselloviruses with Extensive Genomic Variations. *J. Virol.* **2020**, *94* (4). https://doi.org/10.1128/JVI.01624-19.

(54) Collins, A. J.; Whitaker, R. J. CRISPR Comparison Toolkit: Rapid Identification, Visualization, and Analysis of CRISPR Array Diversity. *CRISPR J.* **2023**, *6* (4), 386–400. https://doi.org/10.1089/crispr.2022.0080.

Supplementary Files

This is a list of supplementary files associated with this preprint. Click to download.

- SupplementatryInformation.docx